24th INTERNATIONAL CONGRESS ON SOUND AND VIBRATION
23–27 July 2017, London

ICSV24
23-27JULY 2017
LONDON CALLING

SIMULATING FLAME RESPONSE TO ACOUSTIC EXCITATION FOR AN INDUSTRIAL GAS TURBINE COMBUSTOR

Yu Xia, Aimee S. Morgans, William P. Jones
Department of Mechanical Engineering, Imperial College London, London, UK
email: yu.xia13@imperial.ac.uk

Xingsi Han
College of Energy & Power Engineering, Nanjing University of Aeronautics and Astronautics, Nanjing, China

This work numerically investigates the unsteady heat release rate response of a full-scale industrial gas turbine combustor to acoustic perturbations. The combustor contains a lean technically-premixed methane/air flame. Two large eddy simulation solvers are compared, the first being the in-house code BOFFIN which employs a reduced 15-step chemical reaction mechanism; the second is based on the open-source CFD toolbox OpenFOAM and applies both 2-step and 4-step reaction mechanisms. Both are incompressible codes, exploiting the fact that the flame responds to hydrodynamic perturbations excited by the acoustics. For the unforced flow-field, the simulation results agree well with the experiments. The flame heat release rate responses are calculated by applying a harmonic forcing velocity upstream to the flame across two forcing amplitudes and eight forcing frequencies. The obtained frequency responses of flame are known as flame describing functions, which are different between the solvers used, especially on their gains. This indicates that for combustors with industrial complexity, more detailed chemistry mechanisms may be necessary. The phase lags of the flame describing functions generally decrease linearly with forcing frequency, being almost independent of the forcing amplitude and the solver used.

Keywords: Gas turbine combustor, Flame describing function, Chemical reaction mechanism, BOFFIN, OpenFOAM

1. Introduction

For both aero-engines and land-based gas turbines, low NOx emission combustion is preferred, which can be achieved using lean premixed combustion technology [1]. However, this is highly susceptible to thermoacoustic instabilities, caused by a two-way coupling between acoustic disturbances and unsteady flame heat release rate. These result in large amplitude oscillations and eventually the fatigue failure of devices. The acoustic perturbations can be modelled by a low-order network model (e.g., [2, 3]) or a Helmholtz solver (e.g., [4]), both assuming that the acoustic waves behave linearly, and interact with an " acoustically-compact" flame whose thickness is small compared to the dominant acoustic wavelengths. The flame region can then be represented as a "thin flame sheet" [5], with its heat release rate response to upstream acoustic perturbations captured by a weakly nonlinear "flame describing function (FDF)". The FDF assumes that the heat release response frequency matches the acoustic forcing frequency, but with a gain [6] and phase change [7] that depend on forcing amplitude as well as frequency. Various FDFs have been measured by experiments [6–8] or calculated by large eddy simulations (LES) [9–11] for different laboratory combustors.

Most LES studies of FDFs have been performed using compressible solvers, which are time intensive due to the required small time step. Recently, the fact that the flame responds primarily to hydrodynamic flow disturbances (originally excited by acoustic waves) has been exploited using incompressible LES solvers [12, 13], which are much faster than compressible codes. Thus in this work the incompressible LES is used to obtain the FDFs, defined in frequency domain as:

$$\mathrm{FDF}\left(\omega, \frac{\hat{u}_1(s)}{\overline{u}_1}\right) = \frac{\hat{\dot{Q}}(s)/\overline{\dot{Q}}}{\hat{u}_1(s)/\overline{u}_1}, \tag{1}$$

where the complex variable $s = \sigma + i\omega$, with σ the growth rate and $\omega = 2\pi f$ the angular frequency. $\dot{Q}$ denotes the flame heat release rate, and u_1 denotes the forced velocity perturbation upstream to the flame front, with $\hat{()}$ representing the fluctuations in frequency domain and $\overline{()}$ the mean values. The FDF is a function of both the velocity perturbation frequency, f, and the normalised perturbation amplitude, $|\hat{u}_1(s)/\overline{u}_1|$.

The present work numerically investigates the flame responses to acoustic excitations in an adapted Siemens SGT-100 gas turbine combustor [14–16] (see Fig. 1), for which unforced experimental validation is possible. It consists of a radial swirler entry and a premixing chamber, followed by the main combustion chamber and an exit pipe. The combustion chamber contains large-scale flow features, such as swirl, separation, recirculation and vortex shedding, etc. The fuel is the simplified German Natural Gas (CH_4: 98.97%, CO_2: 0.27%, N_2: 0.753%) [16], operated at two pressures of 3 bar and 6 bar, reaching a global fuel/air equivalence ratio of 0.60 [15]. The gaseous fuel is injected through the swirler entry at temperature 305 K and partially-premixed with the preheated air inflows at 682 K before entering the combustion chamber. The mean mixture velocity and temperature are measured to be 19.40 m/s and 668.47 K respectively at the chamber inlet, with the highest mixture temperature measured to be 1830 K at the mean flame front [15]. The FDFs of this combustor are then calculated using two incompressible (also known as "low Mach number") LES solvers: the first uses the in-house code BOFFIN [17]; the second uses the open-source CFD toolbox OpenFOAM [18]. Reduced chemistry mechanisms for methane/air reaction with different steps are defined: 15 steps for BOFFIN, 2 and 4 steps for OpenFOAM, resulting in three sets of FDFs at 3 bar pressure and two sets of FDFs at 6 bar pressure. The reminder of this paper is organised as follows: the numerical methods and the validation of LES results are presented in Section 2, the obtained numerical FDFs are presented and compared in Section 3, and the conclusions are drawn in the final section.

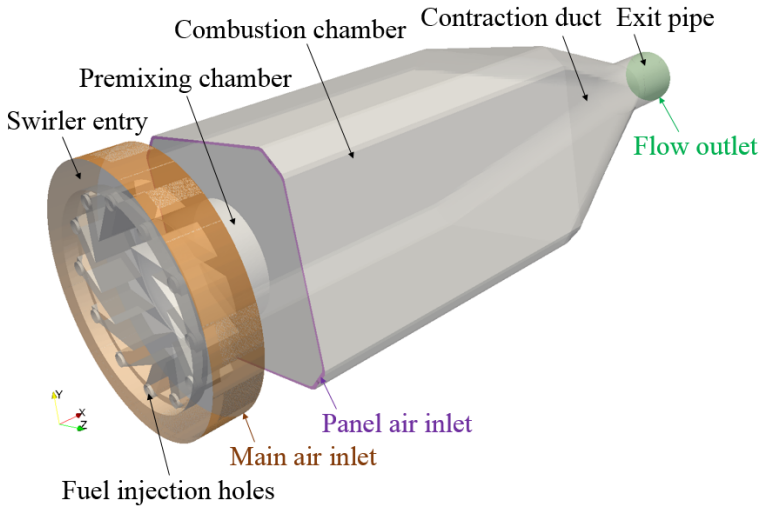

Figure 1: Computational domain of the adapted Siemens SGT-100 gas turbine combustor, containing 8.5 million structured mesh cells.

2. Numerical Methodology

The incompressible version of the in-house code BOFFIN [17, 19] is firstly used for LES, which applies a Favre filter for mass, momentum, species mass fraction and energy conservation equations based on local mesh cells. The code uses a 2nd-order Crank-Nicolson scheme for time derivatives and a 2nd-order central difference scheme for spatial discretisations. The dynamic Smagorinsky model [20] is used to model the sub-grid stress tensor, and the Eulerian stochastic field method [21] is applied to capture the turbulence-combustion interaction, using a series of stochastic fields to solve the probability density functions (PDF) of the species mass fractions plus the enthalpy. Only one stochastic field is used in the present work to reduce computational costs. A reduced 15-step methane/air reaction mechanism is used at both pressures, which involves 19 intermediate species [22]. In order to avoid the solution divergence, a small computational time step of 5×10^{-7} s is used.

The second incompressible LES solver used is the ReactingFOAM solver included in the open-source CFD toolbox OpenFOAM [18]. It uses a 2nd-order Crank-Nicolson method for time integration, and applies a 2nd-order Gaussian method for convection and divergence terms. The constant Smagorinsky model [23] is used to model the sub-grid scale turbulence, and the Partially-Stirred Reactor (PaSR) model [24] is used to model the filtered chemical reaction rates based on both combustion and turbulent mixing time-scales. Two types of reduced CH_4/air reaction mechanism are used at 3 bar pressure, with 2 steps [25] and 4 steps [26] respectively, both involving 7 intermediate species. The 2-step chemistry is also used for all simulations at 6 bar pressure. Finally, a larger time step of 5×10^{-6} s is used by OpenFOAM.

For both LES solvers, the computational domain (see Fig. 1) and the mesh are the same. The main domain inlet corresponds to the swirler entry, including the main air inlet and the fuel injection holes. The panel air inlet has a small amount of preheated air entering the combustion chamber through the front edges. All the air and fuel inflow velocities are prescribed as uniform. The domain outlet locates at the combustion chamber exit plane, where the velocity gradient is set as zero and no backward flow exists. All the other boundaries are set as non-slip adiabatic walls. The computational domain is split into 240 blocks, and each block is meshed with structured cells, giving a total number of 8.5 million structured mesh cells. The turbulent reacting flow-field simulated by two LES solvers at 3 bar pressure is shown in Fig. 2. The axial flow velocity field obtained by BOFFIN (Fig. 2a) contains more details compared to OpenFOAM results (Fig. 2b-c), and its heat release rate distribution (Fig. 2d) also reveals more detailed flame structure including wrinkling and stretching. The reason is that BOFFIN uses a more detailed (15-step) reaction mechanism. Overall, the main features of the flow-field and the flame simulated by both solvers are generally similar and agree well with the experiments [14, 15].

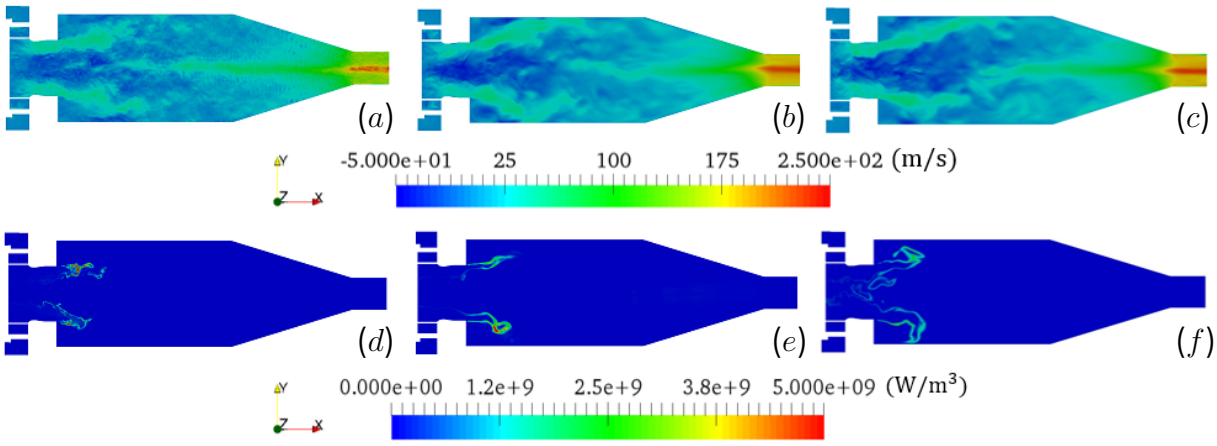

Figure 2: Instantaneous contours of (a-c) axial flow velocity and (d-f) flame heat release rate per unit volume, all on the symmetry plane of $z = 0$, simulated by (a,d) BOFFIN using 15-step reaction mechanism and (b,c,e,f) OpenFOAM using (b,e) 4-step and (c,f) 2-step reaction mechanisms. All simulations are performed at 3 bar pressure.

The radial profiles of mean and RMS flow properties are compared at axial location $x = 43$ mm,

closely upstream to the flame front (see Fig. 3). It is observed that both BOFFIN and OpenFOAM simulation results match well with the experimental data [16], although small differences exist in some RMS variables (e.g., Fig. 3h). The LES results at 6 bar pressure also match the measurements well, indicating that both LES solvers are able to capture the flow-field with sufficient accuracy.

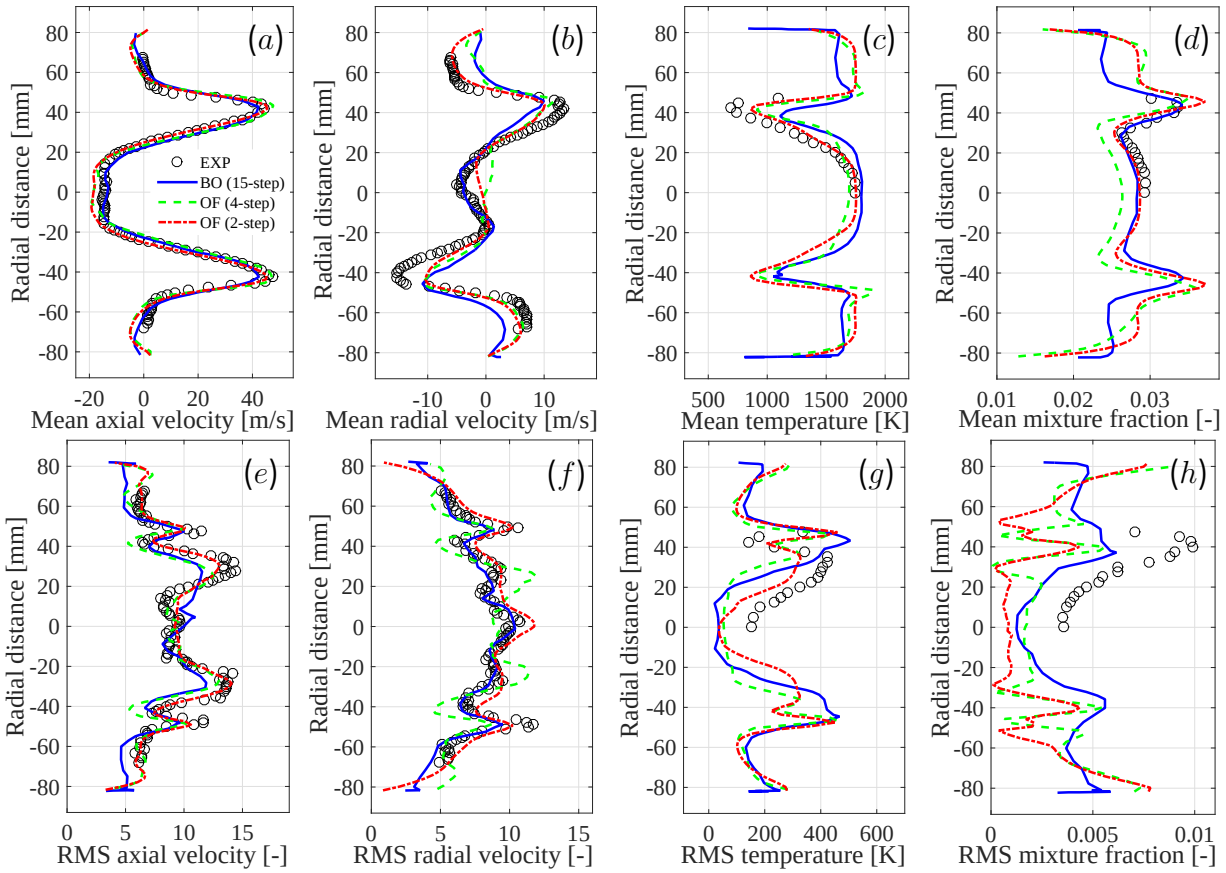

Figure 3: Radial profiles of (a-d) mean and (e-h) fluctuating (RMS) flow variables at an axial location (x = 43 mm) closely upstream to flame front, obtained by BOFFIN-LES (solid lines), OpenFOAM-LES (dashed lines for 4-step reaction and dash-dotted lines for 2-step reaction), and experimental measurements [16] (circles). The origin x = 0 locates at the combustion chamber entrance.

In order to determine the flame describing functions (FDFs), a sinusoidal fluctuation of the air inflow velocity, U'_{air}, is superimposed on the uniform air inflow at the main swirler entry, giving:

$$U_{air} = \overline{U}_{air} \cdot [1 + A_U \cdot \sin(2\pi \cdot f_U \cdot t)], \tag{2}$$

where f_U denotes the forcing frequency, and $A_U = |U'_{air}/\overline{U}_{air}|$ denotes the normalised forcing amplitude, with the mean velocity $\overline{U}_{air}$ = 4.99 m/s. Two levels of forcing (A_U = 0.1 and 0.2) across eight frequencies (f_U = 200 – 1500 Hz) are selected, which are varied independently and result in a total of 16 forcing cases. Each case is simulated by both LES solvers at two operating pressures. The detailed information of these cases are summarised in Table 1.

Table 1: Cases with different velocity forcing frequencies (f_U) and normalised forcing amplitudes (A_U), simulated by both BOFFIN and OpenFOAM LES solvers at 3 bar and 6 bar pressure.

Case No.	1	2	3	4	5	6	7	8
A_U [-]				0.1				
f_U [Hz]	200	300	400	500	600	800	1000	1500
Case No.	9	10	11	12	13	14	15	16
A_U [-]				0.2				
f_U [Hz]	200	300	400	500	600	800	1000	1500

3. Results and Discussion

For each of the velocity forcing cases, the flame's responding heat release rate field, $\dot{Q}(x, y, z)$, is spatially-integrated and averaged over the domain volume, Ω, leading to a spatially-averaged heat release rate, $\langle \dot{Q} \rangle = \left[\oint_\Omega \dot{Q}(x, y, z) d\Omega \right] / \Omega$. The value of $\langle \dot{Q} \rangle$ is calculated at each time step and recorded for at least 15 – 20 forcing cycles after the initial transients died away. Since the weakly nonlinear theory assumes that the main heat release rate response occurs at the forcing frequency, f_U, the time-variation of $\langle \dot{Q} \rangle$ can be approximated as:

$$\langle \dot{Q} \rangle = \overline{\langle \dot{Q} \rangle} \cdot \left[1 \ + A_{\dot{Q}} \cdot \sin(2\pi \cdot f_U \cdot t + \phi_{\dot{Q}}) \right], \tag{3}$$

where $A_{\dot{Q}} = \text{FFT}(\langle \dot{Q} \rangle' / \overline{\langle \dot{Q} \rangle})$ denotes the normalised fast Fourier transform (FFT) amplitude of heat release rate fluctuation, $\langle \dot{Q} \rangle'$, at forcing frequency f_U. $\phi_{\dot{Q}}$ denotes the phase lag between the forcing velocity and the responding heat release rate (cf. Eq. (2)), equal to the maximum cross-correlation magnitude between the time-variations of U_{air} and $\langle \dot{Q} \rangle$.

Two illustrative forcing cases are shown in Fig. 4, obtained by OpenFOAM LES at 3 bar pressure using a 2-step chemistry [25]. The first case (Fig. 4a) is forced at a low frequency (f_U = 200 Hz) while the second (Fig. 4b) is forced at a higher frequency (f_U = 1000 Hz), both with a low forcing amplitude, A_U = 0.1. The main spectral peak of $\langle \dot{Q} \rangle$ appears at the forcing frequency for the f_U = 200 Hz case, but not for that with f_U = 1 kHz. The same phenomena were observed at 6 bar pressure, and also for 4-step chemistry OpenFOAM LES and BOFFIN LES simulations. This means the weakly nonlinear theory is valid at lower forcing frequencies up to around 1 kHz. The flame is well-known to act as a low-pass filter [7], with its heat release response decaying with frequency. At the higher forcing frequencies (e.g., 1 kHz), the heat release response to upstream acoustic excitation is of the same order as that to the highly turbulent flow, as confirmed by the unforced heat release rate spectra shown in Fig. 4.

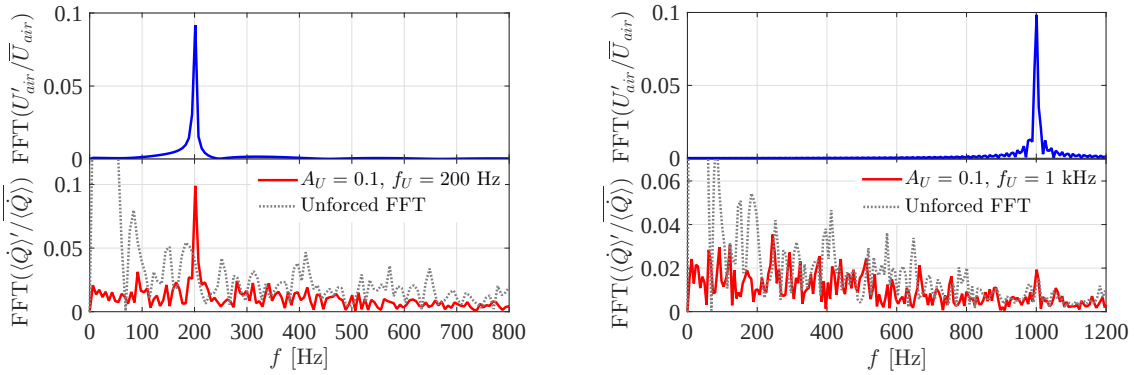

(a) A_U = 0.1, f_U = 200 Hz (b) A_U = 0.1, f_U = 1000 Hz

Figure 4: Fast Fourier transform (FFT) spectra of the normalised forcing velocity $U'_{air}/\overline{U}_{air}$ (blue lines) and heat release rate $\langle \dot{Q} \rangle' / \overline{\langle \dot{Q} \rangle}$ (red lines), forced at (a) f_U = 200 Hz and (b) f_U = 1000 Hz with forcing amplitude A_U = 0.1. The unforced heat release rate FFT spectra are indicated by grey dotted lines. Both cases are simulated by OpenFOAM LES at 3 bar pressure with a 2-step chemistry.

In order to obtain the weakly non-linear FDFs, the normalised amplitude, $A_{\dot{Q}}$, and the phase lag, $\phi_{\dot{Q}}$, of the heat release rate response should always refer to their values at the forcing frequency, f_U. The FDF is then expressed in frequency domain as:

$$\text{FDF} = \frac{\text{FFT}\left(\langle \dot{Q} \rangle' / \overline{\langle \dot{Q} \rangle} \right)}{\text{FFT}\left(U'_{air} / \overline{U}_{air} \right)} = G \cdot e^{i\phi}, \tag{4}$$

where $G = A_{\dot{Q}}/A_U$ is the FDF's gain, and $\phi = \phi_{\dot{Q}} \pm N \cdot 2\pi$ denotes the phase, with N a suitable integer. The values of G and ϕ are obtained by both solvers for all 16 velocity forcing cases, using all three reaction mechanisms at 3 bar pressure. Since the 4-step chemistry is invalid at high pressures, only the 2-step chemistry is applied in OpenFOAM at 6 bar. A 20th-order polynomial fitting is then performed for all the gains and phases over the frequency for each forcing level A_U, resulting in the completed numerical FDFs as shown in Fig. 5.

It is observed that at both pressures, the FDFs simulated by BOFFIN using a 15-step chemistry generally have much lower gains than the OpenFOAM-FDFs using simpler chemistries, indicating that the reduced chemistry with fewer steps may result in higher heat release rate fluctuations. For all of the FDFs, the gain G generally decreases with the increasing forcing amplitude A_U due to the nonlinear saturation, while the phase ϕ linearly decreases with the forcing frequency and does not rely on the forcing level. This is because ϕ is generally inversely proportional to the fuel/air premixture velocity and thus not highly affected by the combustion model or chemistry used. The same phenomenon was observed in a previous experiment [27].

In order to understand the differences between BOFFIN and OpenFOAM-FDFs, two additional BOFFIN cases have been performed with 8 stochastic fields at 3 bar pressure. The first is forced at $f_U = 500$ Hz and $A_U = 0.1$ (Fig. 5a), and the other at $f_U = 600$ Hz and $A_U = 0.2$ (Fig. 5b). Both cases give very similar FDF gain and phase values compared to those obtained by one stochastic field, indicating that the reduced number of stochastic fields may be not the reason for the FDF differences.

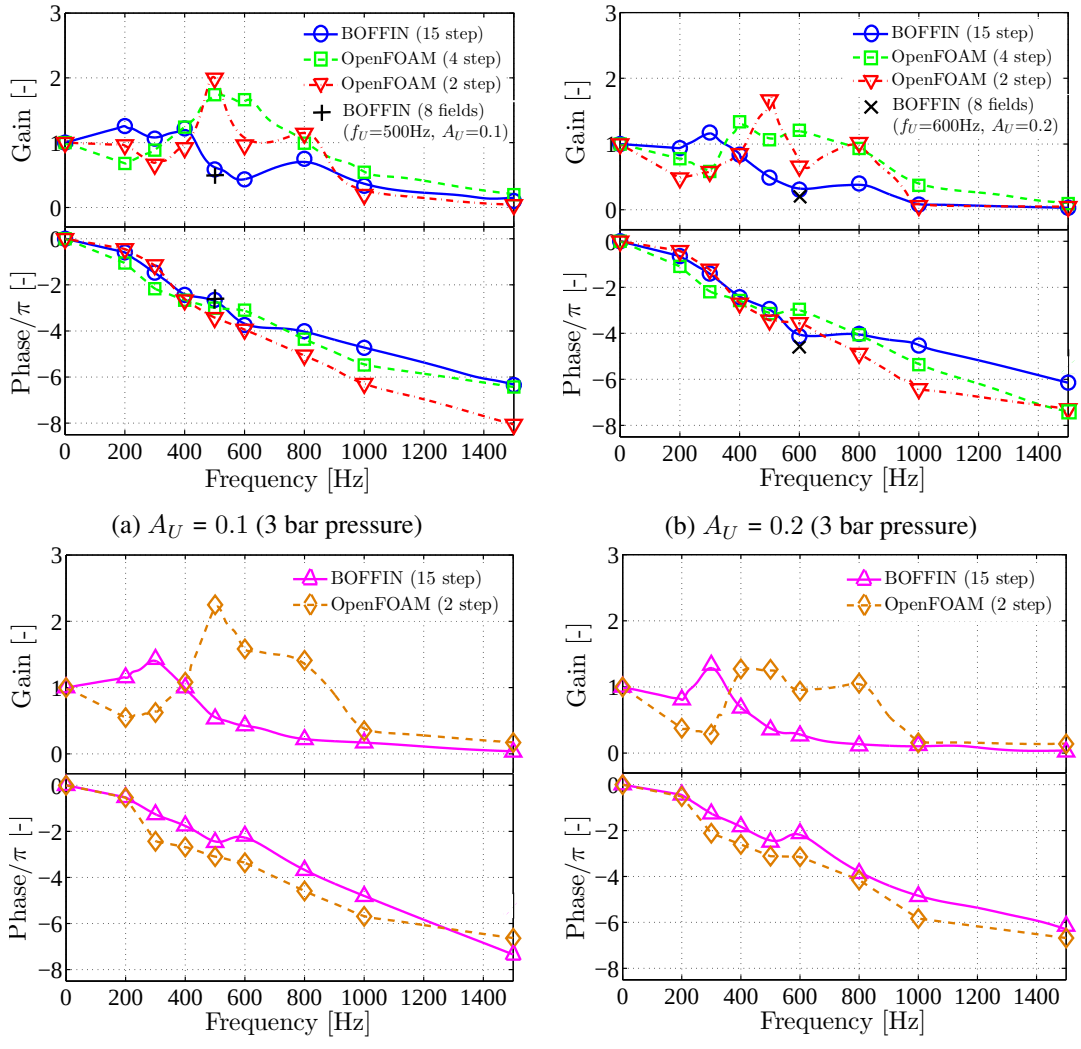

(a) $A_U = 0.1$ (3 bar pressure)

(b) $A_U = 0.2$ (3 bar pressure)

(c) $A_U = 0.1$ (6 bar pressure)

(d) $A_U = 0.2$ (6 bar pressure)

Figure 5: Polynomially-fitted flame describing functions (FDFs) simulated by BOFFIN and OpenFOAM at (a-b) 3 bar and (c-d) 6 bar pressure, with forcing level (a,c) $A_U = 0.1$ and (b,d) $A_U = 0.2$. Two 8-stochastic-field BOFFIN forcing cases at 3 bar pressure are marked with (+) for $f_U = 500$ Hz and $A_U = 0.1$ and (×) for $f_U = 600$ Hz and $A_U = 0.2$.

4. Conclusion

The heat release response to acoustic excitations for a flame in a full-scale industrial gas turbine combustor has been numerically studied. Two incompressible LES solvers, BOFFIN and OpenFOAM, are used to calculate the flame heat release rates under a series of upstream forcing velocities, resulting in the weakly nonlinear flame describing functions (FDFs) at two operating pressures. A reduced 15-step methane/air reaction mechanism is used by BOFFIN, with OpenFOAM using simpler 2-step and 4-step chemistries at 3 bar but only 2-step chemistry at 6 bar pressure. The accuracy of the LES unforced flow-field is validated by comparing to the experimental data. The obtained FDFs are different on gains between two LES solvers, most likely due to the different chemistries and combustion models used. The FDF phases are more independent and linearly decrease with frequency. The reason for these differences will be investigated more fully in future work.

Acknowledgment

The authors appreciate the help from Dr G. Bulat and Dr J. Rogerson from Siemens UK, and acknowledge the financial support from the Siemens Industrial Turbomachinery Ltd., the ERC Starting Grant (grant No: 305410) ACOULOMODE (2013-2018), the National Natural Science Foundation of China (grand no: 51606095), the Jiangsu Provincial Natural Science Foundation of China (grand no: BK20160794), the EPSRC CDT in Fluid Dynamics across Scales and the Department of Mechanical Engineering at Imperial College London. Access to HPC facilities at Imperial College London and via the UK's ARCHER are also highly appreciated.

REFERENCES

1. Moore, M. J. NOx Emission Control in Gas Turbines for Combined Cycle Gas Turbine Plant, *Proceedings of the Institution of Mechanical Engineers, Part A: Journal of Power and Energy*, **211** (1), 43–52, (1997).

2. Paschereit, C. O., Flohr, P. and Schuermans, B. Prediction of Combustion Oscillations in Gas Turbine Combustors, *AIAA Paper*, **2001-0484**, 1–13, (2001).

3. Li, J. and Morgans, A. S. Time Domain Simulations of Nonlinear Thermoacoustic Behaviour in a Simple Combustor Using a Wave-Based Approach, *Journal of Sound and Vibration*, **346**, 345–360, (2015).

4. Laera, D., Prieur, K., Durox, D., Schuller, T., Camporeale, S. and Candel, S. Impact of Heat Release Distribution on the Spinning Modes of an Annular Combustor With Multiple Matrix Burners, *J. Eng. Gas Turbines Power.*, **139** (5), (2017).

5. Marble, F. E. and Candel, S. M. An Analytical Study of the Non-Steady Behavior of Large Combustors, *Proceedings of the Combustion Institute*, **17** (1), 761–769, (1979).

6. Balachandran, R., Ayoola, B. O., Kaminski, C. F., Dowling, A. P. and Mastorakos, E. Experimental Investigation of the Nonlinear Response of Turbulent Premixed Flames to Imposed Inlet Velocity Oscillations, *Combustion and Flame*, **143** (1), 37–55, (2005).

7. Noiray, N., Durox, D., Schuller, T. and Candel, S. A Unified Framework for Nonlinear Combustion Instability Analysis Based On the Flame Describing Function, *Journal of Fluid Mechanics*, **615**, 139–167, (2008).

8. Durox, D., Schuller, T., Noiray, N. and Candel, S. Experimental Analysis of Nonlinear Flame Transfer Functions for Different Flame Geometries, *Proceedings of the Combustion Instiute.*, **32** (1), 1391–1398, (2009).

9. Roux, S., Lartigue, G., Poinsot, T., Meier, U. and Bérat, C. Studies of Mean and Unsteady Flow in a Swirled Combustor Using Experiments, Acoustic Analysis, and Large Eddy Simulations, *Combustion and Flame*, **141** (1), 40–54, (2005).

10. Krediet, H. J., Beck, C. H., Krebs, W., Schimek, S., Paschereit, C. O. and Kok, J. B. W. Identification of the Flame Describing Function of a Premixed Swirl Flame From LES, *Combustion Science and Technology*, **184** (7-8), 888–900, (2012).

11. Han, X. and Morgans, A. S. Simulation of the Flame Describing Function of a Turbulent Premixed Flame Using an Open-Source LES Solver, *Combustion and Flame*, **162** (5), 1778–1792, (2015).

12. Febrer, G., Yang, Z. and McGuirk, J. J. A Hybrid Approach for Coupling of Acoustic Wave Effects and Incompressible LES of Reacting Flows, *Proceedings of the 47th AIAA/ASME/SAE/ASEE Joint Propulsion Conference & Exhibit*, pp. 6127–6144, (2011).

13. Han, X., Li, J. and Morgans, A. S. Prediction of Combustion Instability Limit Cycle Oscillations by Combining Flame Describing Function Simulations with a Thermoacoustic Network Model, *Combustion and Flame*, **162** (10), 3632–3647, (2015).

14. Stopper, U., Aigner, M., Ax, H., Meier, W., Sadanandan, R., Stöhr, M. and Bonaldo, A. PIV, 2D-LIF and 1D-Raman Measurements of Flow Field, Composition and Temperature in Premixed Gas Turbine Flames, *Experimental Thermal and Fluid Science*, **34** (3), 396–403, (2010).

15. Stopper, U., Meier, W., Sadanandan, R., Stöhr, M., Aigner, M. and Bulat, G. Experimental Study of Industrial Gas Turbine Flames Including Quantification of Pressure Influence on Flow Field, Fuel/Air Premixing and Flame Shape, *Combustion and Flame*, **160** (10), 2103–2118, (2013).

16. Bulat, G., Jones, W. P. and Marquis, A. J. NO and CO Formation in an Industrial Gas-Turbine Combustion Chamber Using LES with the Eulerian Sub-Grid PDF Method, *Combustion and Flame*, **161** (7), 1804–1825, (2014).

17. Jones, W. P., di Mare, F. and Marquis, A. J., (2012), LES-BOFFIN: User's Guide. Imperial College London, London, UK.

18. Weller, H. G., Tabor, G., Jasak, H. and Fureby, C. A Tensorial Approach To Computational Continuum Mechanics Using Object-Oriented Techniques, *Computers in Physics*, **12** (6), 620–631, (1998).

19. Jones, W. P. and Prasad, V. N. LES of a Turbulent Premixed Swirl Burner Using the Eulerian Stochastic Field Method, *Combustion and Flame*, **159** (10), 3079–3095, (2012).

20. Piomelli, U. and Liu, J. Large-Eddy Simulation of Rotating Channel Flows Using a Localized Dynamic Model, *Physics of Fluids (1994-present)*, **7** (4), 839–848, (1995).

21. Valiño, L. A Field Monte Carlo Formulation for Calculating the Probability Density Function of a Single Scalar in a Turbulent Flow, *Flow, Turbulence and Combustion*, **60** (2), 157–172, (1998).

22. Sung, C., Law, C. and Chen, J.-Y. Augmented Reduced Mechanisms for NO Emission in Methane Oxidation, *Combustion and Flame*, **125** (1), 906–919, (2001).

23. Smagorinsky, J. General Circulation Experiments with the Primitive Equations: I. the Basic Experiment, *Monthly Weather Review*, **91** (3), 99–164, (1963).

24. Chen, J. Y. Stochastic Modeling of Partially Stirred Reactors, *Combustion Science and Technology*, **122** (1-6), 63–94, (1997).

25. Westbrook, C. K. and Dryer, F. L. Chemical Kinetic Modeling of Hydrocarbon Combustion, *Progress in Energy and Combustion Science*, **10** (1), 1–57, (1984).

26. Abou-Taouk, A., Farcy, B., Domingo, P., Vervisch, L., Sadasivuni, S. and Eriksson, L. E. Optimized Reduced Chemistry and Molecular Transport for Large Eddy Simulation of Partially Premixed Combustion in a Gas Turbine, *Combustion Science and Technology*, **188** (1), 21–39, (2016).

27. Palies, P., Durox, D., Schuller, T. and Candel, S. Nonlinear Combustion Instability Analysis Based On the Flame Describing Function Applied to Turbulent Premixed Swirling Flames, *Combustion and Flame*, **158** (10), 1980–1991, (2011).